

A Heat-Sinking Self-Referencing Raman Probe

Nicholas Djeu and Yutaka Shimoji

MicroMaterials, Inc., Tampa, FL 33637 USA

ABSTRACT

A novel heat-sinking, self-referencing fiber optic Raman probe having a sapphire fiber probe head is described. The laser heating effect in a GaAs wafer (on a PTFE platform) has been measured with the probe in both a noncontact proximity mode and the contact mode. The GaAs/PTFE composite was selected to simulate the thermal conductivity of animal tissues. It was found that for the same laser power delivered to the wafer, the temperature rise in the contact mode was only 42% of that in the proximity mode. Additionally, a demonstration of the self-referencing capability of the probe is also presented.

Index Headings: Raman probe; Fluorescence probe; Self-referencing Raman probe; Self-referencing fluorescence probe; Fiber optic Raman probe; Fiber optic fluorescence probe; Heat-sinking Raman probe; Heat-sinking fluorescence probe; Subcutaneous Raman probe; Subcutaneous fluorescence probe.

INTRODUCTION

The quantitative measurement of Raman emission intensity requires the use of a reference, because the strength of the detected signal depends on a number of factors – such as the power of the excitation laser beam incident on the sample, the sample illumination geometry, the coupling of the emission from the sample to the spectrometer, and the detection efficiency of the spectrometer – which in general cannot be accurately determined. The challenge is particularly severe in the case of fiber optic Raman measurement systems, since the signal can often change even with movements in the input and output optical fibers. To surmount this difficulty, a standard internal to the sample may be used.^{1,2} Alternately, the standard may be incorporated into the Raman measurement system itself.³⁻⁵ This latter self-referencing approach has the advantage that it is universally applicable to all samples. In Ref. 3 a diamond film was deposited onto the end of the fiber optic probe, the Raman emission of which served as the standard. But the polycrystalline film drastically reduced the optical power incident on the sample as well as the coupling of the Raman emission from the sample back into the probe. Ref. 4 also made use of diamond as the standard, but in the form of a small single crystal embedded in a glass tip formed at the end of the fiber optic probe. However, since the diamond particle had to be offset from the main light path in order to avoid excessive scattering, the ratio of the Raman signals from the diamond and the sample still varied with changes in the optical alignment of the system.

Whereas in Refs. 3 and 4 optical fibers were used in coupling the excitation light from the laser to the sample and the Raman emission from the sample to the spectrometer, the external standard was incorporated into a free space Raman measurement system in Ref. 5. In that work, the excitation laser beam was made to form two foci, the first of which being situated inside a sapphire window and the second inside the sample. However, the Raman emission from the

sapphire was much weaker than that from the samples tested. This necessitated the use of a long collection time of 300 s. Even then, the application of the “second derivative variance minimalization” spectral subtraction procedure was needed to achieve the desired signal-to-noise level.⁶ The Raman probe reported here represents an improvement on this earlier sapphire reference approach.

Another limitation of Raman spectroscopy as a diagnostic tool is the heating of the sample.⁷⁻¹⁰ With 300 mW of 1,064 nm laser power incident on sulfur, it was found that the sample temperature increased from ambient to 400 K.⁸ Biodegradation can be expected to occur with much smaller increases. The authors of Ref. 9 were able to reduce the heating effect by rotating the sample. But this option is not always available, as when the spatial variation of the Raman spectrum is of primary interest. It will be shown that the Raman probe presented in this paper is capable of reducing the laser heating effect at a fixed position when used in the contact mode, as a result of the high thermal conductivity of sapphire.

THE RAMAN PROBE

In this paper we describe the performance of a self-referencing fiber optic Raman probe with heat-sinking capability, which incorporates a single crystal sapphire optical fiber. The probe can be used in either a contact mode or a noncontact proximity mode. The elements of the probe are shown schematically in Fig. 1. The sapphire fiber in the probe head is oriented along the c-axis, and measures 0.4 mm in diameter and 7.8 cm in length. It serves as an external standard much like the sapphire window employed in Ref. 5. As shown in Fig. 2, the distal end of the fiber is encased in a hypodermic pipetting needle with a blunt end, while its proximal end terminates in a fiber optic connector which is detachable from the body of the probe. As a result of the much

longer interaction length through the sapphire material, the Raman signal produced in this arrangement is correspondingly increased compared to that obtained in Ref. 5. For the c-axis fiber, three dominant Raman peaks at 417.4, 576.7, and 750.0 cm^{-1} with FWHM of 2.2, 3.2, and 9.5 cm^{-1} respectively are observed.^{11,12} Since the excitation laser powers entering and leaving the sapphire fiber bear a fixed relationship and the Raman signal from the sample shares the same optical path on its way to the spectrometer as that produced by the sapphire fiber, the intensity of the latter serves as a reliable reference for the intensity of the former. In other words, the recorded Raman emissions from the sapphire fiber and the sample will change in the same proportion with variations in the laser power or the transmissions of the input and output optical fibers connected to the probe.

EXPERIMENTAL METHOD

An undoped GaAs wafer measuring 1 mm x 1 mm with a thickness of 0.2 mm served as the sample. The temperature dependence of the photoluminescence of GaAs has been studied previously.¹³ It was shown that the peak of the photoluminescence exhibited a sensitive dependence on the temperature, and therefore can be used to determine the temperature of the material. A diode laser at 785 nm served as the excitation source. The spectral width of the laser was 0.15 nm. At this wavelength, the excitation light is essentially completely absorbed in the 0.2 mm thick wafer.¹⁴ For the laser heating studies, the GaAs wafer was placed on a block of PTFE with a thermal conductivity of 0.25 W/m/K.

The emphasis of this work is on the heat sinking feature of the sapphire fiber Raman probe. Although the self-referencing aspect of the probe will also be illustrated, it will not be analyzed in great detail. The reason is that the photoluminescence of GaAs is very broad, overlapping the

sapphire Raman peaks on its short wave side. This makes the material ill-suited for a good demonstration of the self-referencing feature. A quantitative application of the latter has been presented earlier for the measurement of ethanol in ethanol-water mixtures.¹⁵

EXPERIMENTAL RESULTS

Since the temperature dependent photoluminescence data in Ref. 13 were obtained for GaAs slightly doped with Si and only two spectra were shown in the temperature range of interest to us, it was necessary to first record the photoluminescence spectra for our undoped GaAs wafer at a larger number of temperatures. For that purpose, the wafer was placed on an aluminum block, which in turn rested on a hotplate. The temperature of the aluminum block was monitored with a K-type thermocouple inserted into a thermal well with less than 1 mm diameter on the side of the block approximately 1.5 mm below the top surface. The thermocouple junction was positioned directly under the wafer.

For these photoluminescence calibration measurements the Raman probe was positioned with the end of the sapphire fiber approximately 2 mm above the GaAs wafer. To ensure that the laser beam itself produced negligible heating effect, the current was made sufficiently low so that further reduction produced no measurable change in the position of the emission maximum. The spectrum obtained at ambient temperature is shown in Fig. 3. The three sapphire Raman peaks are seen to be considerably wider than indicated earlier, especially the two with the smaller Raman shifts. This was due to the fact that the spectrometer used was uncooled. Thus, even for the longest integration time of 6.5 s smoothing had to be implemented to enable the precise measurement of the photoluminescence peak wavelength. This did not noticeably alter the overall GaAs emission spectrum, but broadened the sapphire Raman peaks appreciably. The

variation of the photoluminescence peak wavelength with temperature between 25 °C and 55 °C is shown in Fig. 4. It is seen that the data can be well fitted to a straight line in this temperature range.

Since for a given experimental arrangement multiple measurements had to be made at different diode laser power levels, it was necessary to first determine how the laser power exiting the sapphire fiber varied with the current setting of the power supply. This presented a slight problem, since the digital current readout of the power supply had a resolution of only 0.01 A. For some current readings the measured optical power can change by more than 5% within this window. An effort was made to set the current control knob at a position corresponding to the middle of the 0.01 A window. The dependence of the laser power exiting the Raman probe as a function of the diode laser's operating current is shown in Fig. 5. It can be seen that some scatter in the measured power nevertheless resulted in spite of the care taken. This amount of uncertainty will also be present in the laser heating measurements made subsequently.

For the laser heating investigations the GaAs wafer was placed on a block of PTFE. First a series of measurements of the photoluminescence peak wavelength at different laser operating current levels were made with the Raman probe positioned so that the end of the sapphire fiber was approximately 1 mm away from the wafer. Then a second set of data were taken with the end of the sapphire fiber contacting the wafer. Both sets of results are shown in Fig. 6. Since the laser power delivered to the wafer is proportional to the laser's operating current and an increase in the peak photoluminescence wavelength corresponds to an increase in the wafer's temperature, the heat sinking effect of the sapphire fiber is immediately evident.

Because the relationship between laser operating current and output power from the Raman probe as well as that between the measured photoluminescence peak wavelength and the temperature of the wafer are linear, Fig. 6 can readily be converted to one showing how the wafer's temperature changes with the laser power delivered to it. However, one must take note of the fact that the measured laser power shown in Fig. 5 is not the same as the power delivered to the wafer. In the case where the probe was used in the proximity mode, the power actually delivered to the wafer was reduced by the Fresnel loss at the air/GaAs interface. On the other hand, in the contact mode it was reduced by the difference between the Fresnel loss at the $\text{Al}_2\text{O}_3/\text{GaAs}$ interface and that at the $\text{Al}_2\text{O}_3/\text{air}$ interface. The plots for wafer temperature vs. delivered laser power, after the Fresnel loss corrections have been made, are shown in Fig. 7. The two straight-line fits to the proximity mode and contact mode data sets should intersect at zero laser power for constant ambient temperature and perfect data. The fact that they almost do gives us a measure of confidence in the quality of the data. The graph shows that for the maximum laser power delivered to the wafer of 34 mW in the proximity mode the temperature rise was 35 °C. By drawing a horizontal line through the power point of 48 mW, it is seen that for the same heating effect one can deliver 2.4 times more laser power to the wafer in the contact mode. Viewed another way, for the same laser power of 34 mW delivered to the GaAs wafer, the temperature rise in the contact mode is only 42% of that in the proximity mode.

The spectrum shown in Fig. 3, as were all the other spectra used in generating the data in Figs. 4 and 6, were obtained by subtracting the dark spectrum recorded with the laser beam blocked. However, by using the Raman spectrum generated by the sapphire fiber alone (i.e., with the output laser light incident on just air) as the “dark” spectrum, one can readily see how the self-referencing feature of the probe works. This was done in the acquisition of Figs. 8a and

8b recorded with the GaAs wafer positioned 2 mm below the probe head. In this case, the “dark” spectrum was obtained with the laser operating near the low end of the 0.38 A range. The spectrum in Fig. 8a was taken at exactly the same current setting. The appearance of the three sapphire Raman peaks there indicates that either the laser power had drifted up a little or the mode pattern of the laser output had changed in such a way that slightly more power was being coupled into the fiber leading to the probe. Turning the current knob on the power supply to a position near the high end of the 0.38 A range resulted in the spectrum shown in Fig. 8b. It is seen that the photoluminescence peak height increased by approximately 8%. The percentage increase in the sapphire peaks can be estimated with reference to the “dark” spectrum to be near 6%, in fair agreement with the change in the GaAs signal.

A quantitative correlation between the sapphire reference signal and the GaAs photoluminescence signal was made difficult in this work by the extensive wing of the latter. However, in the absence of such interference a quantitative application of the self-referencing feature of the probe can be readily implemented. We have demonstrated in our laboratory that the sapphire fiber Raman probe can be used to determine the ethanol concentration in ethanol-water mixtures to an accuracy of 1%. This was possible by working with just the peak heights of the Raman lines.

DISCUSSION AND CONCLUSION

First it should be noted that, while photoluminescence was used to demonstrate the heat-sinking and self-referencing features of the probe described here, the same results should hold in the case of Raman emission, albeit the Raman signal would generally be weaker. For example, the 880 cm^{-1} Raman signal from ethanol in the contact (i.e., immersion) mode is only slightly

larger than the weakest Raman peak from the sapphire fiber shown in Fig. 3. Nevertheless, for an integration time of 6.5 s and excitation laser power of 50 mW, approximately 2,000 counts can be obtained. Thus, with a spectrometer capable of longer integration times, significantly stronger Raman signals can be expected even without any increase in the laser power.

Next we examine more closely the experimental arrangement employed in order to facilitate the extrapolation of the present results to other situations. Since the area of the GaAs wafer was approximately 2.5 times larger than that of the probe head and the thermal conductivity of GaAs is more than 2 orders of magnitude larger than that of PTFE, the thermal energy deposited in the wafer is quickly spread throughout its volume. Then it is transferred to the PTFE block across the entire 1 mm x 1 mm surface area. Thus, the effective thermal conductivity of the wafer/PTFE composite is significantly larger than that of the PTFE. In fact, in a one-dimensional picture it would be a factor of 2.5 larger.

If we take the effective thermal conductivity of the wafer/PTFE composite to be twice that of the PTFE, then it would be nearly the same as that of most biological materials (the thermal conductivity of water being 0.6 W/m/K). Since the thermal degradation of tissues in Raman spectroscopy is a major concern, the ability to deliver 140% more laser power than a non-contact Raman probe for the same amount of heating is a significant advantage. Moreover, the self-referencing capability would permit the measurement of the absolute rather than relative magnitudes of the sample's Raman peaks. By polishing the end of the probe head at an angle, one can turn it into a penetrating hypodermic needle. Then the probe would be suitable for subcutaneous applications. A word should also be said about the effect of the strength of absorption at the excitation laser wavelength. Since the diameter of the sapphire fiber used was

0.4 mm, it is clear that the reported results should hold so long as the absorption length is comparable to or less than that.

It is of interest to assess the heat sinking effect of the probe if a standard silica fiber instead of a sapphire fiber had been used to deliver the laser power. The hypodermic needle used had an inside diameter of 0.4 mm and an outside diameter of 0.7 mm. Since the thermal conductivities of sapphire and stainless steel are 35 W/m/K and 14 W/m/K respectively, the stainless steel sheath is responsible for only 45% of the thermal conduction. If the sapphire fiber were to be replaced with a silica fiber with a typical thermal conductivity of just 1.4 W/m/K, the overall heat sinking effect would be reduced by a factor of 2. Additionally, silica fibers have Raman emissions which are both weaker and much broader with an extensive red wing, making them poor standards if self-referencing is also desired.

Finally, we indicate how improvement in the heat sinking capability of the sapphire fiber Raman probe can be made for subcutaneous applications. A standard 22 gauge hypodermic needle has a wall thickness of 0.15 mm, same as that of the pipetting needle sleeve for the 0.4 mm sapphire fiber employed in this work. This regular wall thickness is used for hypodermic needles in order to provide sufficient rigidity in tissue penetration. However, a sapphire fiber with diameter as large as 0.4 mm is by itself already quite rigid. Therefore, one can use for the sleeve a 22 gauge hypodermic tubing with an extra thin wall of 0.075 mm. This will keep the OD of the needle the same and increase its ID to 0.56 mm, permitting the diameter of the sapphire fiber to increase to 0.55 mm. By making this modification of the probe tip, its heat sinking capability should increase by another 30%.

REFERENCES

1. D.P. Strommen and K. Nakamoto. *Laboratory Raman Spectroscopy*. New York: Wiley, 1984.
2. S. Song and S.A. Asher. "Internal Intensity Standards for Heme Protein UV Resonance Raman Studies: Excitation Profiles of Cacodylic Acid and Sodium Selenate". *Biochemistry*. 1991. 30:1199-1205.
3. H. Xiao, S. Dai, J.P. Young, C.S. Feigerle, and A.G. Edwards. "Quantitative Raman Spectral Measurements Using a Diamond-Coated All-Silica Fiber Optic Probe". *Appl. Spectrosc.* 1998. 52(4):626-628.
4. X. Zheng, W. Fu, S. Albin, K.L. Wise, A. Javey, and J.B. Cooper. "Self-Referencing Raman Probes for Quantitative Analysis". *Appl. Spectrosc.* 2001(4). 55:382-388.
5. R.N. Favors, Y. Jiang, Y.L. Loethen, and D. Ben-Amotz. "External Raman Standard for Absolute Intensity and Concentration Measurements". *Rev. Sci. Instrum.* 2005:033108.
6. Y.L. Loethen, D. Zhang, R.N. Favors, S.B.G. Basiaga, and D. Ben-Amotz. "Second Derivative Variance Minimization Method for Automated Spectral Subtraction". *Appl. Spectrosc.* 2004. 58(3):272-278.
7. S.J.A. Pope and Y.D. West. "Use of the FT Raman Spectrum of Na_2MoO_4 to Study Sample Heating by the Laser". *Spectrochim. Acta Part A*. 1995. 51:2011-2017.
8. N.A. Marigheto, E.K. Kemsley, J. Potter, P.S. Belton, and R.H. Wilson. "Effects of Sample Heating in FT-Raman Spectra of Biological Materials". *Spectrochim. Acta Part A*. 1996. 52:1571-1579.

9. J. Johansson, S. Pettersson, and L.S. Taylor. "Infrared Imaging of Laser Induced Heating during Raman Spectroscopy of Pharmaceutical Solids". *J. Pharm. Biomed. Anal.* 2002. 30:1223-1231.
10. J. Zhang, Z. Feng, M. Li, J. Chen, Q. Xu, Y. Lian, and C. Li. "Raman Spectroscopic Investigation of Solid Samples Using a Low-Repetition-Rate Pulsed Nd:YAG Laser as the Excitation Source". *Appl. Spectrosc.* 2007. 61(1):38-47.
11. S.P.S. Porto and S.S. Krishnan. "Raman Effect of Corundum". *J. Chem. Phys.* 1967. 47(3):1009-1012.
12. G.H. Watson, W.B. Daniels, and C.S. Wang. "Measurement of Raman Intensities and Pressure Dependence of Phonon Frequencies in Sapphire". *J. Appl. Phys.* 1981. 52(2):956-958.
13. V.I. Osinsky and N.N. Winogradoff. "Excitation and Temperature Dependence of Band Edge Photoluminescence in Gallium Arsenide". *Phys Rev. B.* 1971. 3(10):3341-3346.
14. H.C. Casey, Jr., D.D. Sell, and K.W. Wecht. "Concentration Dependence of the Absorption Coefficient of n- and p- Type GaAs between 1.3 and 1.6 eV". *J. Appl. Phys.* 1975. 46(1):250-257.
15. N. Djeu. "Sapphire Fiber Self-Referencing Raman Probe". Paper (poster) presented at: PITTCON 2013. Philadelphia; March 17-21, 2013.

FIGURE CAPTIONS

Fig.1 Schematic of sapphire fiber Raman probe, shown together with the excitation laser and the fiber optic spectrometer.

Fig.2 Photograph of sapphire fiber probe head.

Fig.3 Uncorrected emission spectrum obtained at room temperature. The three narrow peaks on the left are Raman lines from the sapphire fiber, while the broad peak on the right is the photoluminescence from the GaAs wafer. It should be noted that the sensitivity of the spectrometer falls off rapidly towards longer wavelengths.

Fig.4 Measured variation of GaAs photoluminescence peak wavelength with temperature.

Fig.5 Laser power exiting the sapphire fiber vs. diode laser operating current.

Fig.6 Peak wavelength of photoluminescence from the GaAs wafer vs. diode laser operating current. The circles represent data obtained with the sapphire fiber 1 mm from the wafer, and the squares with the sapphire fiber in contact with wafer.

Fig.7 GaAs wafer temperature vs. laser power delivered to it after correction for Fresnel losses have been made.. The symbols have the same meanings as in Fig. 7.

Fig.8 Emission spectra obtained using the sapphire fiber Raman signal as the “dark” spectrum. See text for conditions under which the spectra in (a) and (b) were recorded.

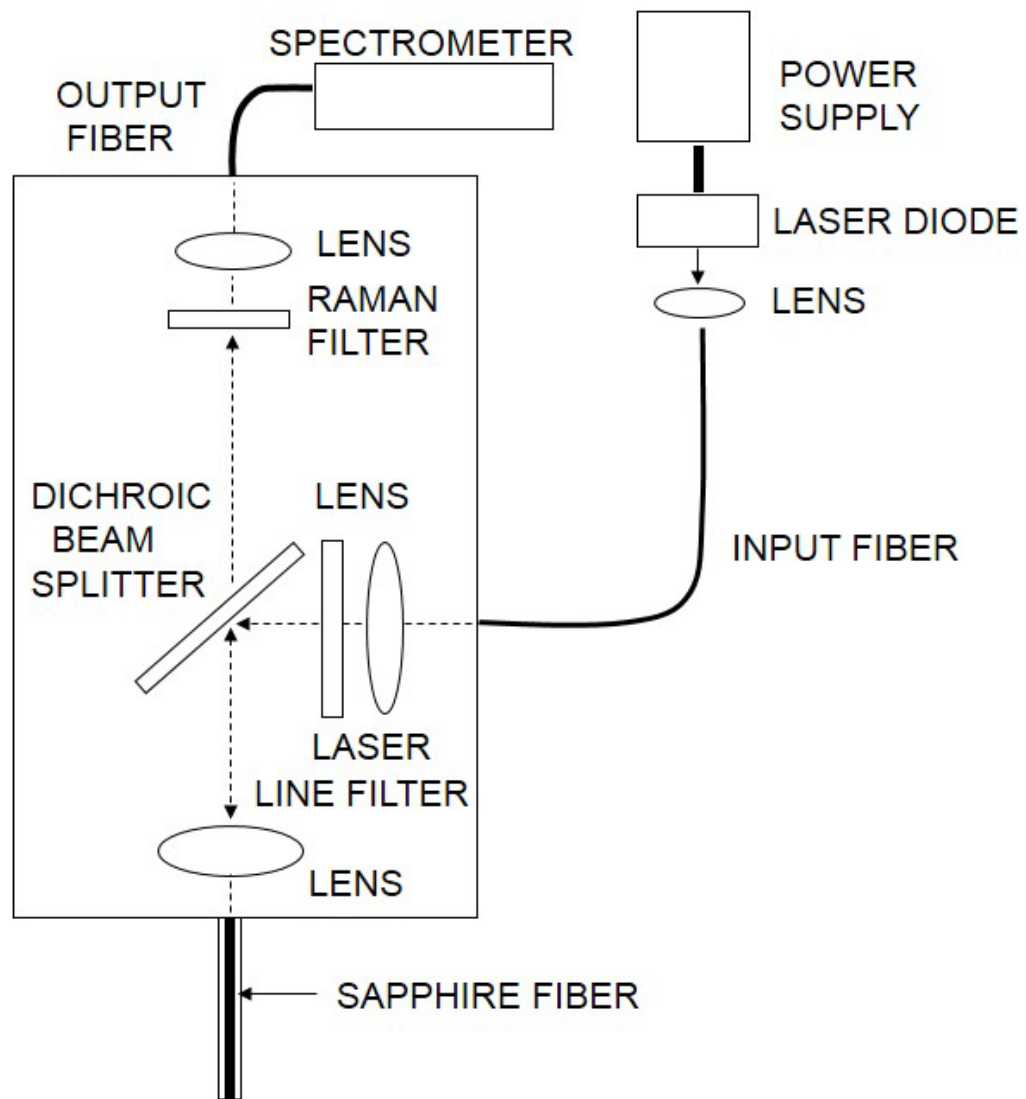


FIG. 1



FIG. 2

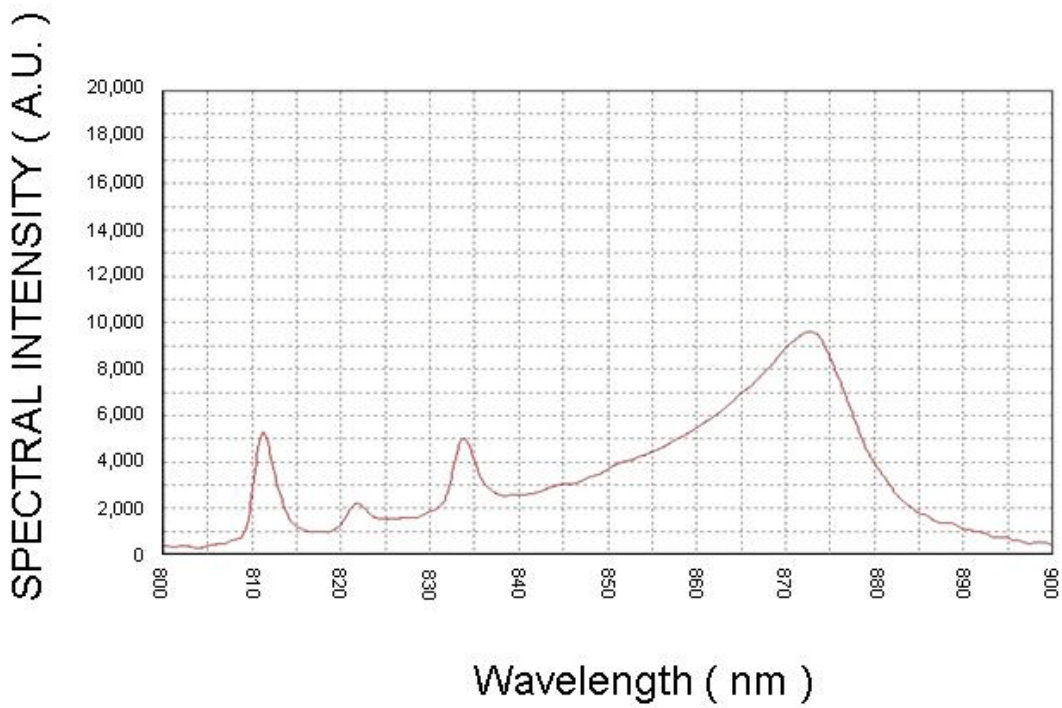


FIG. 3

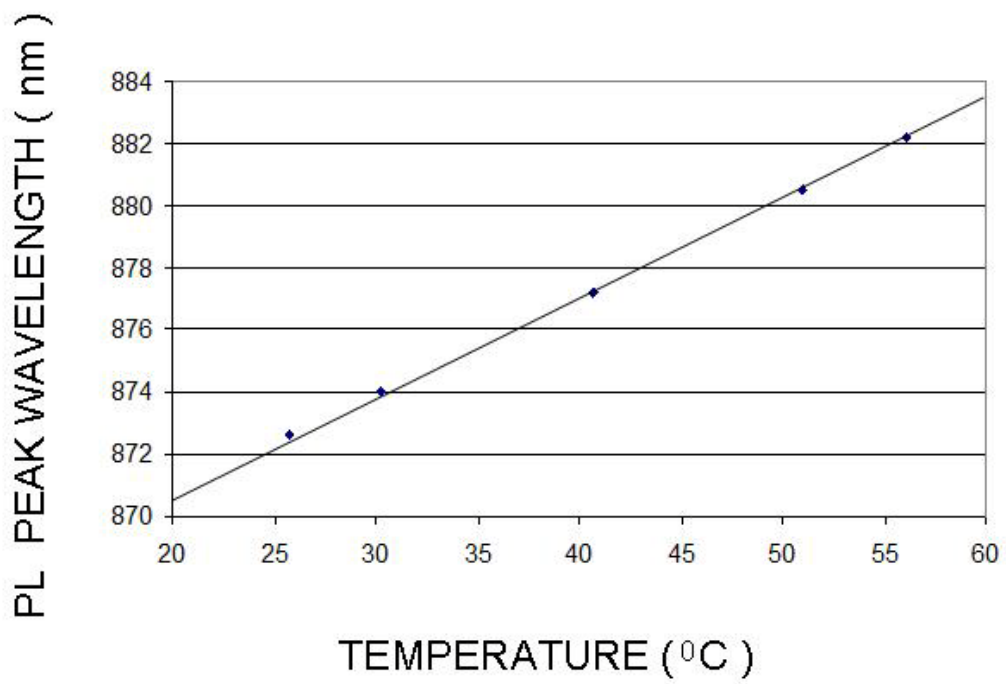


FIG. 4

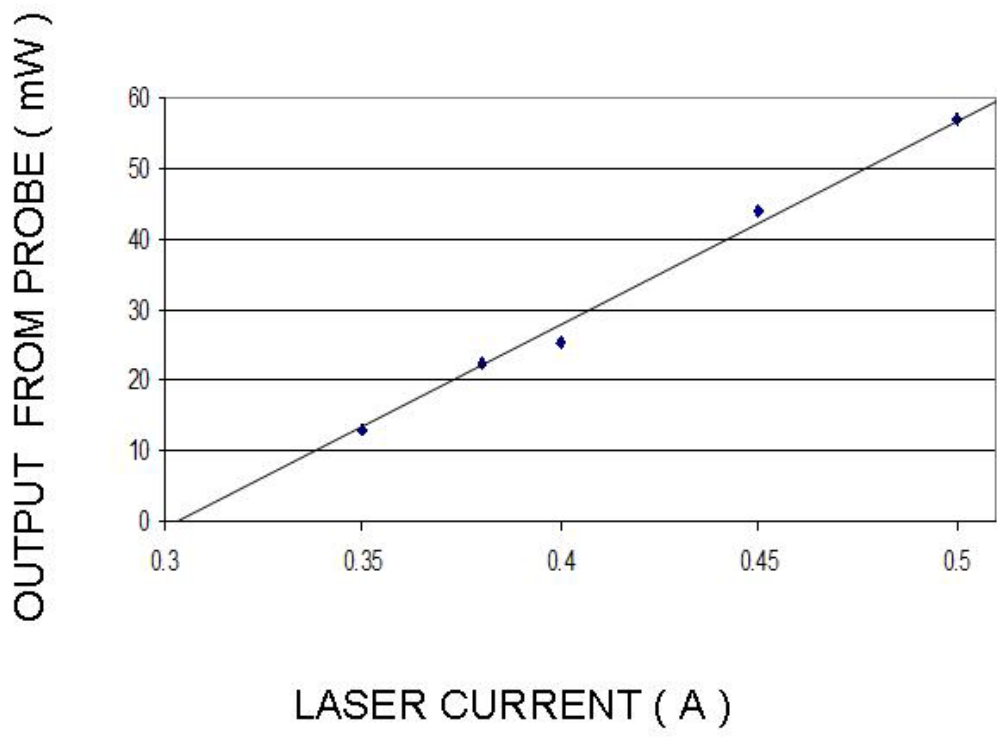


FIG. 5

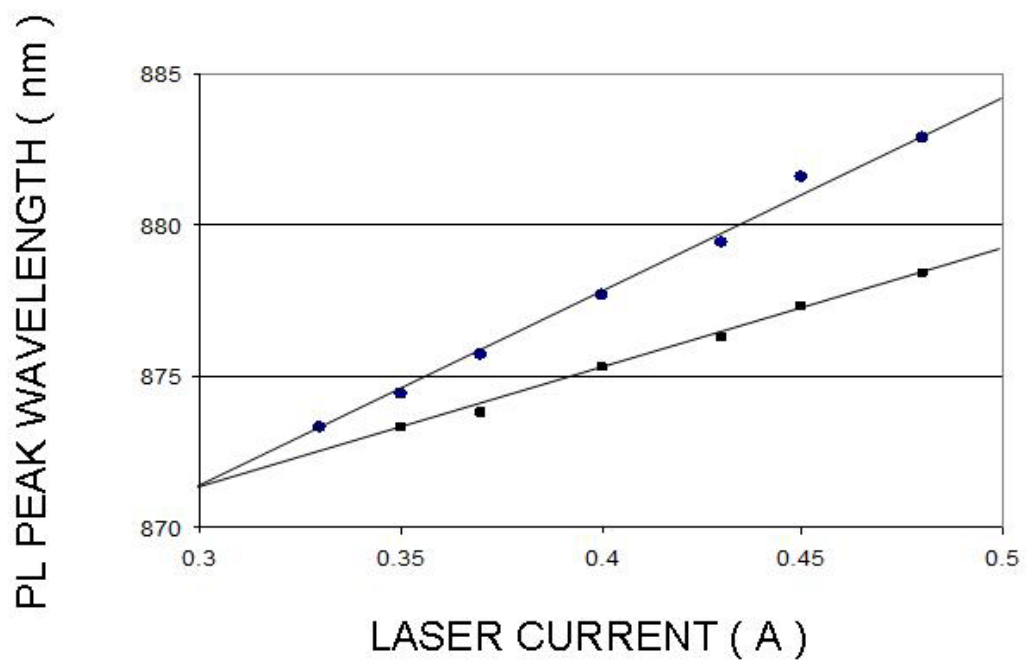


FIG. 6

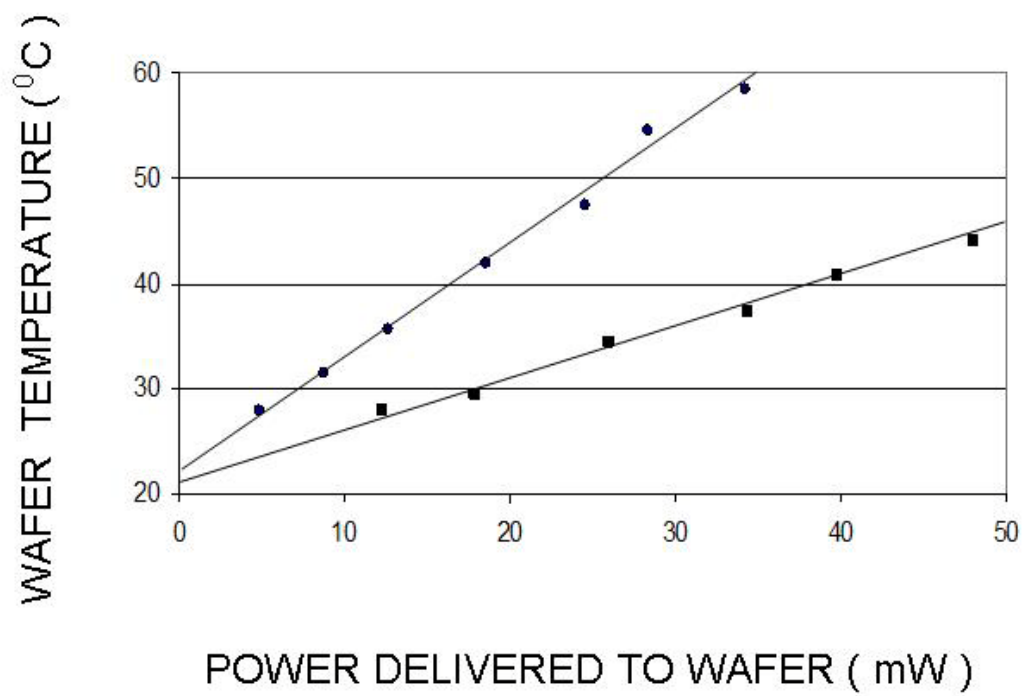
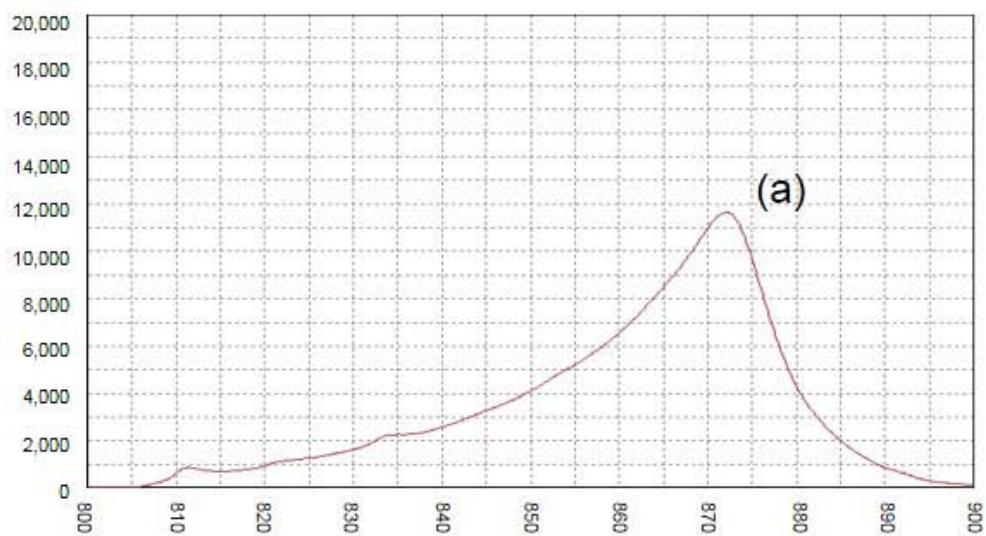


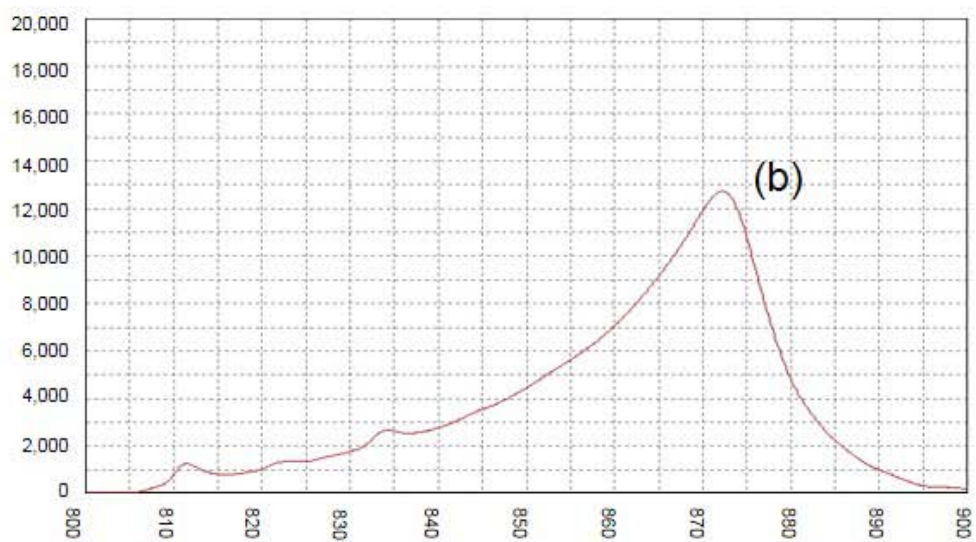
FIG. 7

SPECTRAL INTENSITY (A.U.)



Wavelength (nm)

SPECTRAL INTENSITY (A.U.)



Wavelength (nm)

FIG. 8